Analytical study of flow field and heat transfer of a non-Newtonian fluid in an axisymmetric channel with a permeable wall

G. A. Sheikhzadeh[a], M. Mollamahdi[a*] and M. Abbaszadeh[a]

[a]Mechanical Engineering Department, University of Kashan, Kashan, Iran

Abstract

In this study, the momentum and energy equations of laminar flow of a non-Newtonian fluid are solved in an axisymmetric porous channel using the least square and Galerkin methods. The bottom plate is heated by an external hot gas, and a coolant fluid is injected into the channel from the upper plate. The arising nonlinear coupled partial differential equations are reduced to a set of coupled nonlinear ordinary differential equations using stream function. These equations can be solved using the different numerical method. The numerical solution is conducted using fourth order Rung-Kutta method. With comparing the results obtained from the analytical and numerical methods, a good adaptation can be seen between them. It can also be observed that the results of the Galerkin method have further conformity with the numerical results and the Galerkin method is simpler than the least square method and requires fewer computations. The effects of Reynolds number, Prandtl number and power law index of non-Newtonian fluid is examined on flow field and heat transfer. The results show that Nusselt number increases by increasing Reynolds number, Prandtl number, and power law index.

Nomenclature

A,B	Symmetric kinetic matrices	u_r, u_z	Velocity components in r and z direction
c_p	Specific heat at constant pressure (Jkg-1K-1)	V	Velocity of cooling injection fluid
C_n	Wall temperature coefficient	x_k	General coordinates
F	Velocity function		**Greek symbols**
$\bar{k}$	Coefficient of thermal conductivity (Wm^{-1}K^{-1})	$\delta a_m/\delta x_n$	Acceleration gradient
N	Power law index in the temperature distribution function	$\delta u_m/\delta x_n$	Velocity gradient
Nu	Nusselt number	η	Dimensionless coordinate component in the z direction
P	Pressure (Pa)	ρ	Density (kgm^{-3})
Pr	Prandtl number	τ_{ij}	The components of the stress tensor
$q_n(\eta)$	Temperature function	φ	Dissipation function
Re	Reynolds number	k_1	Non-Newtonian fluid viscosity coefficients
T	Temperature (K)	ψ	Stream function (m^{2}s^{-1})

*Corresponding author
email address: mahdimollamahdi@gmail.com*

1. Introduction

The non-Newtonian fluids have a lot of applications in industrial processes and engineering. The non-Newtonian fluids have a lot of applications in industrial processes and engineering. Extraction of petroleum and production of papers, glasses, crystals, plastic sheets and biological applications, paints production, asphalts, and gels have their usual industrial applications. In recent years, considerable attention is devoted to the use of these fluids in various engineering issues such as their heat transfer problem in the process of cooling, lubricating, and hot rolling. The problem of cooling gas turbine blades to protect them against high temperatures and thus increasing the performance of gas turbines has been studied by researchers in the past years [1-3]. Following the works of the past researchers, Debruge and Han [4] investigated the injection problem of coolant fluid from the surrounding environment with specified characteristics input by power series method and plotted the velocity, temperature and Nusselt profiles for various parameters. Their results show that the power law index, Prandtl number, and the Nusselt number increase through augmentation. The cooling method which they intended, increases energy consumption and reduces efficiency in the turbine. By applying the mechanism in the turbine whereby the drag force is decreased, it is possible to reduce energy consumption and increase the efficiency. The use of certain types of non-Newtonian fluids because of less drag force for cooling gas turbine blades is recommended by Kurtcebe and Erim [5]. They investigated the non-Newtonian viscoelastic fluid flow in an axisymmetric channel, numerically. Their results indicate that by increasing the viscosity of the non-Newtonian fluid, the friction coefficient reduces and the Nusselt number increases. Esmaeilpour et al. [6] examined Homotopy analysis method for the heat transfer of a non-Newtonian fluid flow in an axisymmetric channel with a porous wall. Their results represent that the calculated temperatures distribution in the channel using the analytical and Homotopy method are analogous. Hosseini et al. [7] investigated the same issue by Optimal

Homotopy Asymptotic Method (OHAM). They showed that the Nusselt number increases with an increase in the Reynolds number, Prandtl number and power law index. Ashorynejad et al. [8] studied the same problem using Parameterized Perturbation Method (PPM) and evaluated the effects of the Reynolds number, Prandtl number and power law index on the Nusselt number. Their results also indicate a direct relationship between the Nusselt number and these parameters.

Although in the recent years, analytical methods were used successfully in various scientific fields [9–15], the exact or approximate analytical solutions have been regarded due to their better physical understanding the effects of various physical parameters. When the analytical solution of the entire problem is impossible or very difficult, analytical-approximate methods such as the weighted residuals methods are used. The most popular of these methods is the least square and Galerkin method. Initial works performed by these methods can be noted in numerous cases. Stern and Rasmussen [16] solved a third order linear differential equation using collocation method. Vaferi et al. [17] investigated the eventuality of using the orthogonal collocation method to solve diffusivity equations in the radial transient flow system. Hendi and Albugami [18] solved a Fredholm–Volterra integral equation using collocation and Galerkin methods. Recently the least square method was used by Aziz and Bouaziz [19] to prognosticate the performance of the longitudinal fins. They found that the least square method is simpler than other analytical methods. Hatami et al. [20] used the least square and numerical methods to analyze the flow and heat transfer of nanofluids between contracting rotating disks. They investigated the effects of the nanoparticle volume fraction, rotational Reynolds number, injection Reynolds number, and expansion ratio on flow and heat transfer. Their results indicate that as the parameter related to the permeability of the wall increases temperature profile increases and the point of maximum radial velocity shifts towards the middle of two disks. Hatami et al. [21] simulated heat transfer and flow analysis

for a non-Newtonian third grade nanofluid flow in the porous medium of a hollow vessel in the presence of a magnetic field. They demonstrated that by increasing the MHD parameter, velocity profiles decrease due to magnetic field effect. Hatami et al. [22] studied two-phase Nanofluid condensation and heat transfer analysis over a vertical plate under gravity and between two parallel plates under magnetic force using Least Square Method and Rung-Kutta numerical method. They illustrated that TiO_2-water and Ag-water nanofluid have maximum boundary layer thicknesses and Nusselt number, respectively. Mosayebidorcheh et al. [23] investigated nano-bioconvection flow containing both nanoparticles and Gyrotactic microorganisms in a horizontal channel using the modified least square method. Their results represent that Thermophoresis number has little effect on temperature distribution.

By a precise review, it can be found out that a lot of advertency is dedicated to the use of analytical-approximate methods to solve problems in recent years. In these solutions, the equations of flow and heat transfer are turned to the nonlinear ordinary differential equations using similarity transformation. Then, the analytical-approximate methods are used to solve them. Simplicity, lack of truncation, and round-off errors are the advantages of these methods over the numerical methods. Nowadays, several analytical-approximate methods are being offered where each of these methods has advantages and disadvantages.

The purpose of this study is to investigate the laminar flow of non-Newtonian fluid in an axisymmetric channel with permeable walls using least square and Galerkin methods. The conformity of the results of the least square and Galerkin analytical-approximate methods with Rung-Kutta numerical method is checked, and the effect the Reynolds number, Prandtl number, power law index, and non-Newtonian fluid characteristic parameter on the Nusselt number are considered.

2. The governing equations and boundary conditions

In this problem, the flow and heat transfer of a non-Newtonian viscoelastic fluid is studied in an axisymmetric channel with a permeable wall as a model for cooling gas turbines. Figure 1 shows an example of how the turbine blades are chilled.
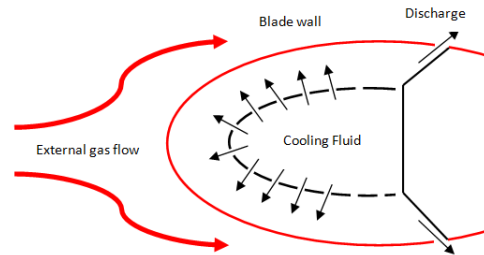

Fig. 1. Schematic illustration of cooling actual turbine blade by coolant fluid.

In order to facilitate the calculation, Fig. 2 shows a schematic of the problem. The r-axis is horizontal, and the z-axis is vertical in the channel. L is the distance between the two-plate of the channel. The porous plate of the channel is at $z = + L$ and the plate in contact with the external hot gases flow is at $z = 0$.
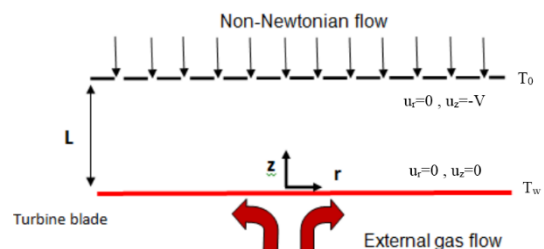

Fig. 2. Schematic view of the geometry of the problem.

The equations of a laminar and steady flow of a non-Newtonian incompressible fluid with constant density in cylindrical coordinates are written in Eqs. (1-3) [4]. The non-Newtonian fluid which is evaluated in this study is from the elastic and non-elastic viscous fluids extracted by Rivlin model [24]. The features of this model are described in reference [4].

$$\frac{\partial(ru_r)}{\partial r} + \frac{\partial(ru_z)}{\partial z} = 0 \qquad (1)$$

$$u_r \frac{\partial(u_r)}{\partial r} + u_z \frac{\partial(u_r)}{\partial z} = -\frac{1}{\rho}\frac{\partial P}{\partial r} +$$

$$\frac{1}{\rho}\left[\frac{\partial \tau_{rr}}{\partial r} + \frac{1}{r}(\tau_{rr} - \tau_{\theta\theta}) + \frac{\partial \tau_{rz}}{\partial z}\right] \qquad (2)$$

$$u_r \frac{\partial(u_z)}{\partial r} + u_z \frac{\partial(u_z)}{\partial z} = -\frac{1}{\rho}\frac{\partial P}{\partial z} +$$

$$\frac{1}{\rho}\left[\frac{\partial \tau_{zr}}{\partial r} + \frac{1}{r}\tau_{rz} + \frac{\partial \tau_{zz}}{\partial z}\right] \qquad (3)$$

In the above equations, u_r and u_z are the velocity components in the r and z directions, V is the velocity of the fluid injected into the channel, ρ and P are the density and pressure. Also, τ_{rr}, τ_{rz}, τ_{zz}, and τ_{zr} are the stress-tensor components of the non-Newtonian fluid. The boundary conditions of the problem are assumed in Eqs. (4 and 5).

$$u_r = 0, u_z = 0 \text{ at z=0} \qquad (4)$$

$$u_r = 0, u_z = -V \text{ at z=+L} \qquad (5)$$

The model which is considered for the non-Newtonian fluid assumes the material homogeneous and isotropic and this model considers the stress components dependent on the displacement, velocity and acceleration variations. The stress components (τ_{ij}) at a point x_k (k =1, 2, 3) and time t is defined as polynomials in the velocity gradient (($\partial u_m/\partial x_n$), ($m$, n=1, 2, 3)) and the acceleration gradients (($\partial a_m/\partial x_n$), ($m,n$=1, 2, 3)) in the Eq. (6) [4].

$$\|\tau_{ij}\| = \Phi_0 I + \Phi_1 A + \Phi_2 A^2 + \Phi_3 B \qquad (6)$$

I is the unit matrices. Φ_1, Φ_2 and Φ_3 are the coefficient of ordinary viscosity, the coefficient of visco-elasticity, and coefficient of cross-viscosity respectively. Generally, Φ_1, Φ_2 and Φ_3 are functions of temperature and materials. In Eq. (6), these parameters are constant. This assumption is correct for many fluids such as polyacrylamide and polyisobutylene [25]. A and

B are symmetric kinematic matrixes defined by Eq. (7) [4].

$$A = \left\|\frac{\partial u_i}{\partial x_j} + \frac{\partial u_j}{\partial x_i}\right\|$$

$$B = \left\|\frac{\partial a_i}{\partial x_j} + \frac{\partial a_j}{\partial x_i} + 2\frac{\partial u_m}{\partial x_i}\frac{\partial u_m}{\partial x_j}\right\| \qquad (7)$$

In Eq. (6), the components of (k =1, 2, 3) are related to the material constant properties. In this case, the stress components are considered in Eqs. (8 to 11) [4].

$$\tau_{rr} = \Phi_1 A_{rr} + \Phi_2 A^2_{rr} + \Phi_3 B_{rr} \qquad (8)$$

$$\tau_{zz} = \Phi_1 A_{zz} + \Phi_2 A^2_{zz} + \Phi_3 B_{zz} \qquad (9)$$

$$\tau_{\theta\theta} = \Phi_1 A_{\theta\theta} + \Phi_2 A^2_{\theta\theta} + \Phi_3 B_{\theta\theta} \qquad (10)$$

$$\tau_{rz} = \Phi_1 A_{rz} + \Phi_2 A^2_{rz} + \Phi_3 B_{rz} \qquad (11)$$

Because the flow is axisymmetric, a stream function that satisfies the continuity equation is defined.

$$\psi = Vr^2 f(\eta) \qquad (12)$$

where $\eta = Z/L$. The velocity components are calculated by Eqs. (13) and (14).

$$u_r = \frac{Vr}{L}f'(\eta) \qquad (13)$$

$$u_z = -2V f(\eta) \qquad (14)$$

By substituting the Eqs. (12) - (14) in Eqs. (1) - (3), Eqs. (15) and (16) are obtained.

$$f'^2 - 2ff'' = -\frac{L^2}{\rho V^2 r}\frac{\partial P}{\partial r} + \frac{\Phi_1}{\rho V L}f''' +$$

$$\frac{\Phi_2}{\rho L^2}(f''^2 - 2f'f''') + \frac{\Phi_3}{\rho L^2}(f''^2 - 2ff^{iv}) \qquad (15)$$

$$4ff' = -\frac{L^2}{\rho V^2}\frac{\partial P}{\partial z} - 2\frac{\Phi_1}{\rho V L}f'' +$$

$$2\frac{\Phi_2}{\rho L^2}\left(14f'f'' + \frac{r^2}{L}f''f'''\right) + 4\frac{\Phi_3}{\rho L^2}$$

$$\left(11f'f'' + ff''' + \frac{r^2}{L}f''f'''\right) \qquad (16)$$

In order to eliminate the pressure term, the Eqs. (15) and (16) are derived with respect to z and r, respectively; subtracting the resulting equations supplies Eq. (17).

$$-2f\,f' = \frac{f^{iv}}{(\rho V L/\mu)} - \left(\Phi_2\Big/\rho L^2\right)$$
$$\left(4f''f''' + 2f'f^{iv}\right) - \left(\Phi_3\Big/\rho L^2\right) \qquad (17)$$
$$\left(4f''f''' + 2f'f^{iv} + 2f\,f^{v}\right)$$

By defining the parameters $k_1 = \Phi_2/\rho L^2$ and $k_2 = \Phi_3/\rho L^2$ as a non-Newtonian fluid characteristics and by considering $k_2 = 0$ and the definition $\mathrm{Re} = \rho V L/\mu$, Eq. (18) is obtained with identified boundary conditions in Eq. (19).

$$f^{iv} + 2\mathrm{Re}f\,f'' + k_1\mathrm{Re}$$
$$\left(4f''f''' + 2f'f^{iv}\right) = 0 \qquad (18)$$

$$f(0)=0,\; f'(0)=0,\; f(1)=1,\; f'(1)=0 \qquad (19)$$

The energy equation for this problem can be expressed as Eqs. (20) and (21).

$$\rho c_p\left(u_r\frac{\partial T}{\partial r} + u_z\frac{\partial T}{\partial z}\right) = \bar{k}\,\nabla^2 T + \varphi \qquad (20)$$

$$\varphi = \tau_{rr}\frac{\partial u_r}{\partial r} + \tau_{\theta\theta}\frac{u_r}{r} +$$
$$\tau_{zz}\frac{\partial u_z}{\partial z} + \tau_{rz}\left(\frac{\partial u_r}{\partial z} + \frac{\partial u_z}{\partial r}\right) \qquad (21)$$

where u_r and u_z are the velocity components in the *r* and *z* directions, respectively, and V is the injection velocity. P, ρ, T, c_p and $\bar{k}$ are the pressure, density, temperature, specific heat, and heat conduction coefficient of fluid, respectively. φ is the dissipation function which is the difference between Newtonian fluid and non-Newtonian fluid energy equation. The where *D* is a differential (partial) operator that is defined as a process when applied to the scalar function *u* produces a function p(y).

temperature distribution on the blade plate (z=0) is considered as Eq. (22).

$$T_w = T_0 + \sum_{n=0}^{\infty} C_n \left(\frac{r}{L}\right)^n \qquad (22)$$

In the distance η away from the blade surface, the fluid temperature can be expressed as Eq. (23).

$$T = T_0 + \sum_{n=0}^{\infty} C_n \left(\frac{r}{L}\right)^n q_n(\eta) \qquad (23)$$

In Eq. (23), T_0 is the temperature of the cooling input fluid (z=L). By defining $\mathrm{Pr} = \nu\Big/\left(\bar{k}\Big/\rho c_p\right)$ and refraining from the effects of the dissipation function [4], the temperature distribution equation with specified boundary conditions is considered as Eqs. (24) and (25).

$$q_n'' - \mathrm{Pr}\,\mathrm{Re}\left(f'\,n\,q_n - 2f\,q_n'\right) = 0$$
$$(n = 0, 2, 3, 4, ...) \qquad (24)$$
$$q_n(0)=1,\quad q_n(1)=0 \qquad (25)$$

3. Weighted residual methods (WRMS)

Weighted residual methods (WRMs) are some of the approximation techniques for solving differential equations. These methods are general and extremely powerful methods for obtaining approximate solutions of ordinary differential equations (ODEs) or partial differential equations (PDEs). Consider the following (partial) differential equation:

$$D\big(u(y)\big) = p(y) \qquad (26)$$

Assume that *u* is approximated by a function *u*, which is a linear combination of basic functions chosen from a linearly autonomous set. That is,

$$u \cong u = \sum_{i=1}^{n} c_i \Phi_i \qquad (27)$$

By substituting Eq. (27) into Eq. (26), the result of the operations usually isn't $p(y)$. Hence an error or residual exists:

$$R(y) = D\big(u(y) - p(y)\big) \neq 0 \qquad (28)$$

Some techniques can be used to properly obtain an approximate function to make the residual as "small" as possible. In this study, the residual is forced to zero in an average sense by setting weighted integrals of residuals to zero. For example, it is imposed:

$$\int_y R(y) W_i(y) dy = 0 \ , i = 1,2,3,..,n \qquad (29)$$

Note that in WRMs, the number of weight functions W_i always equals the number of unknown constants c_i in u. This yields n algebraic equations for the unknown constants c_i. In the weighted residual method, the selection of weight functions affects its performance. Different numerical approximation methods can be obtained by selecting different weight functions. In the following subsections, two methods are discussed.

3.1. Least square method (LSM)

In this method, the summation of all the squares of the residues should be minimized.

$$S = \int_y R(y) R(y) dy = \\ \int_y R^2(y) dy \qquad (30)$$

In order to achieve a minimum of the functional S, the derivatives of S with respect to all the unknown parameters must be zero. That is,

$$\frac{\partial S}{\partial c_i} = 2 \int_y R(y) \frac{\partial R}{\partial c_i} dy = 0 \qquad (31)$$

Comparing with Eq. (29), the weight functions are obtained (as its value should be zero, its constant is not considered).

$$W_i = \frac{\partial R}{\partial c_i} \qquad (32)$$

In order to use the least square method in this problem, the considered function $f(\eta)$ must be satisfied the boundary conditions of the problem. This function is considered as equation (33).

$$f(\eta) = \eta^2 + c_1\big(\eta^2 - \eta^3\big) + \\ c_2\big(\eta^2 - \eta^4\big) + c_3\big(\eta^2 - \eta^5\big) + \\ c_4\big(\eta^2 - \eta^6\big) + c_5\big(\eta^2 - \eta^7\big) + \\ c_6\big(\eta^2 - \eta^8\big) \qquad (33)$$

Table 1. Comparisons the effect of polynomial profiles on the values of f and f '.

Polynomial degree	f(0.5)	f'(0.5)	The relative-error percent of f	The relative-error percent of f '
4	0.509764	1.499999	1.594958	1.055954
5	0.501761	1.516008	0.011332	0.128601
6	0.501818	1.517960	0.004155	0.011476
7	0.501797	1.517786	0.000173	٠.٠٠٣٥٦٩
8	0.501798	1.517809	-	-

In Table 1 a comparison is done between the polynomial profiles in order 4 to 8 for $f(\eta)$ and $f'(\eta)$ and the Re $=0.05$ and $k_1 = 1$ and in $\eta = 0.5$. Because of the relative error variations is too low and close to zero, for profiles with the order

of 7 and 8, a polynomial with the order of 7 is used.
By applying the boundary condition in Eq. (33) and with regard to the obtained relationship from Eq. (31), the coefficient c_1-c_5 are achieved. The residual function for momentum is

obtained by applying Eq. (33) into the Eq. (18). Substituting the residual function into Eq. (31), a set of five equations is obtained and by solving these algebraic equations, the coefficients c_1–c_5 are determined. For example, using the least square method for a non-Newtonian fluid with $K = 0.01$, $\mathrm{Re} = 0.5, \mathrm{Pr} = 1$, the Eq. (34) for momentum is obtained:

$$
\begin{aligned}
f\left(\eta\right) = {} & 3.178381534\eta^2 - \\
& 2.21635865\eta^3 - \\
& 0.08139024555\eta^4 \\
& + 0.06060567405\eta^5 \\
& + 0.09648632388\eta^6 \\
& - 0.03772463507\eta^7
\end{aligned}
\tag{34}
$$

By substituting Eq. (34) into Eq. (24), $q_n\left(\eta\right)$ is obtained by the same process. The approximate function for temperature distribution with regard to satisfying the boundary condition in Eq. (25) is considered as Eq. (35).

$$
\begin{aligned}
q_n\left(\eta\right) = {} & 1 - \eta + c_1\left(\eta - \eta^2\right) + \\
& c_2\left(\eta - \eta^3\right) + c_3\left(\eta - \eta^4\right) \\
& + c_4\left(\eta - \eta^5\right) + c_5\left(\eta - \eta^6\right)
\end{aligned}
\tag{35}
$$

In Table 2 the polynomial profiles in order 2 to 4 are compared to $q(\eta)$ in $\eta = 0.05$ and for the predetermined conditions $\mathrm{Pr} = 1$ and $n = 2$. Due to changes in the relative error is too low and near zero, for profiles with the order of 3 and 4, a polynomial with the order of 3 is used. The $q_n\left(\eta\right)$ is obtained by using the Eq. (36).

$$
\begin{aligned}
q_n\left(\eta\right) = {} & 1 - 1.406208099\eta + \\
& 0.1293490457\eta^2 + \\
& 0.5380673028\eta^3
\end{aligned}
\tag{36}
$$

Table 2. Comparisons of the effect of polynomial profiles on the values of q.

Polynomial degree	q	The relative-error percent of q
2	0.486462	0.051465
3	0.486212	0.014854
4	0.486140	0.00000
5	0.486140	-

3.2. Galerkin method (GM)

The Galerkin method can be viewed as a particular weighted residual method, in which the trial functions used for the approximation of the field function are also used as the weight functions.

$$
W_i = \frac{\partial u}{\partial c_i} \quad i = 1, 2, 3, .., m
\tag{37}
$$

Now, the Galerkin method is used to find the dimensionless velocity profile, ($f(\eta)$). In this case, the weight functions are defined as follows:

$$
\begin{aligned}
& W_1 = \eta^2 - \eta^3, W_2 = \eta^2 - \eta^4, \\
& W_3 = \eta^2 - \eta^5, W_4 = \eta^2 - \eta^6, \\
& W_5 = \eta^2 - \eta^7,
\end{aligned}
\tag{38}
$$

Such as the previous case, by applying the residual function into Eq. (29), a set of algebraic equations appears and by solving them, coefficients c_1–c_4 are achieved. $f(\eta)$ for a second grade non-Newtonian fluid with K=0.01, Re=0.5 and Pr=1 is as follows:

$$
\begin{aligned}
f\left(\eta\right) = {} & 3.176198950\eta^2 - \\
& 2.1969055\eta^3 - \\
& 0.1352125596\eta^4
\end{aligned}
\tag{39}
$$

Considering Eq. (35) as a trial function, weight functions are:

$$
\begin{aligned}
& \omega_1 = \eta - \eta^2, \ \omega_2 = \eta - \eta^3, \\
& \omega_3 = \eta - \eta^4
\end{aligned}
\tag{40}
$$

The dimensionless temperature profile, $q(\eta)$, is obtained as follows:

$$
\begin{aligned}
q_n\left(\eta\right) = {} & 1 - 1.424202217\eta + \\
& 0.1844617494\eta^2 + \\
& 0.4988139827\eta^3 - \\
& 0.259073514\eta^4
\end{aligned}
\tag{41}
$$

4. Result and discussion

In the present study, the Galerkin and the least squares methods are used to obtain analytical

solutions for the laminar flow of a non-Newtonian fluid in an axisymmetric channel with porous walls. At first, a comparison is done between the least square and Galerkin methods with the numerical results of fourth order Rung–Kutta method with 10^{-6} convergence precision. With regard to various parameters of flow and heat transfer in Tables 3 and 4 and Figs. 3-6, these methods are compared and there is a good agreement between the numerical and analytical methods. The tables show that the GM is more accurate and has less error than the LSM. That is why the GM is used to evaluate the effect of Re, Pr, n parameters on profiles f, f' and q_n and the Nusselt number. Error in these tables is calculated by Eq. (42).

$$\text{Error} = 100 \times \frac{\left|\text{Analytical-Numerical}\right|}{\text{Numerical}} \qquad (42)$$

Table 3. Comparison of numerical method and Galerkin and least squares analytical methods in $k_1 = 0.001$ and Re = 0.5 for the velocity component f.

η	Nu_m	LSM	GM	%Error LSM	%Error GM
0	.	.	.	.	.
0.1	0.029553	0.029562	0.029561	0.030453761	0.02707001
0.2	0.1093	0.109307	0.10931	0.006404392	0.009149131
0.3	0.225791	0.225778	0.225794	0.005757537	0.001328662
0.4	0.36562	0.365584	0.36562	0.009846288	0
0.5	0.515638	0.515589	0.51564	0.009502791	0.000387869
0.6	0.663152	0.663107	0.663156	0.006785775	0.00060318
0.7	0.796121	0.796092	0.796124	0.003642662	0.000376827
0.8	0.903307	0.903295	0.903307	0.001328452	0
0.9	0.974386	0.974384	0.974386	0.000205257	0
1	١	١	١	0	0

Table 4. Comparison of numerical method and Galerkin and least squares analytical methods in $k_1 = 0.001$, Re = 0.5, Pr=1 and n=2 for the temperature distribution components q_n.

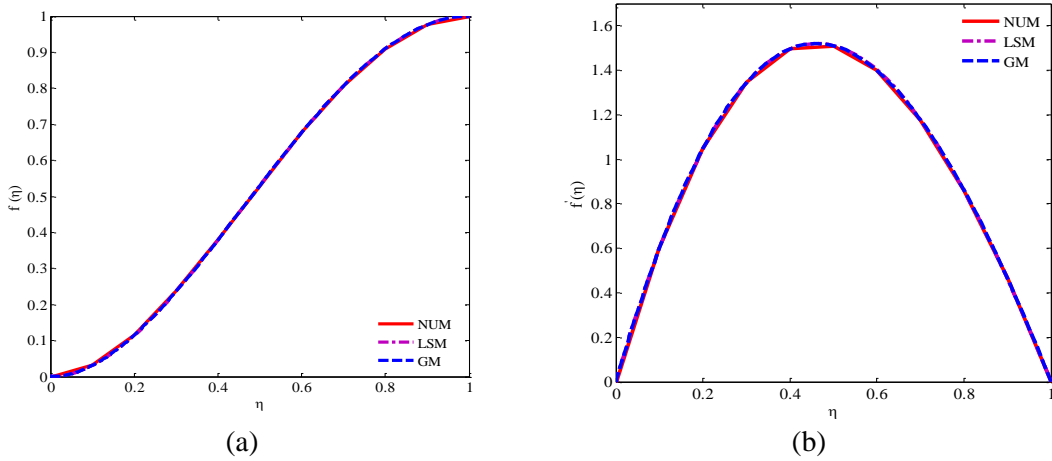| η	Nu_m	LSM	GM	Error LSM	Error GM
0	.	.	.	.	.
0.1	0.859897	0.861184	0.860387	0.149669088	0.056983569
0.2	0.726611	0.727817	0.725918	0.165976017	0.095374279
0.3	0.60071	٠.٦٠٢١٨٩	0.600031	0.246208653	0.113032911
0.4	0.485125	0.48596	0.484592	0.172120587	0.109868591
0.5	0.380174	0.380164	0.380224	0.002630375	0.013151873
0.6	0.286053	0.28521	0.286641	0.294700632	0.205556313
0.7	0.202334	0.200875	0.202976	0.721084939	0.317297142
0.8	0.12797	0.126316	0.128079	1.292490427	0.085176213
0.9	0.061289	0.060057	0.060763	2.01014864	0.858229046
1	١	١	١	.	.

Fig. 3. Comparison of the velocity components of numerical and analytical methods, a) f, b) f ' for k1=0.001 and Re=1.
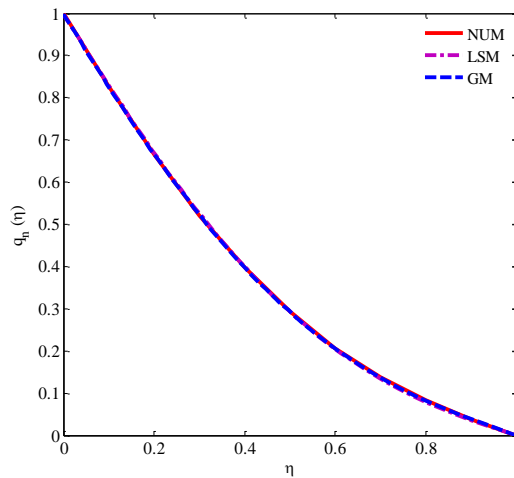

Fig. 4. Comparison of the temperature profiles of numerical and analytical methods (q_n), for k_1=0.001 and Re=1.
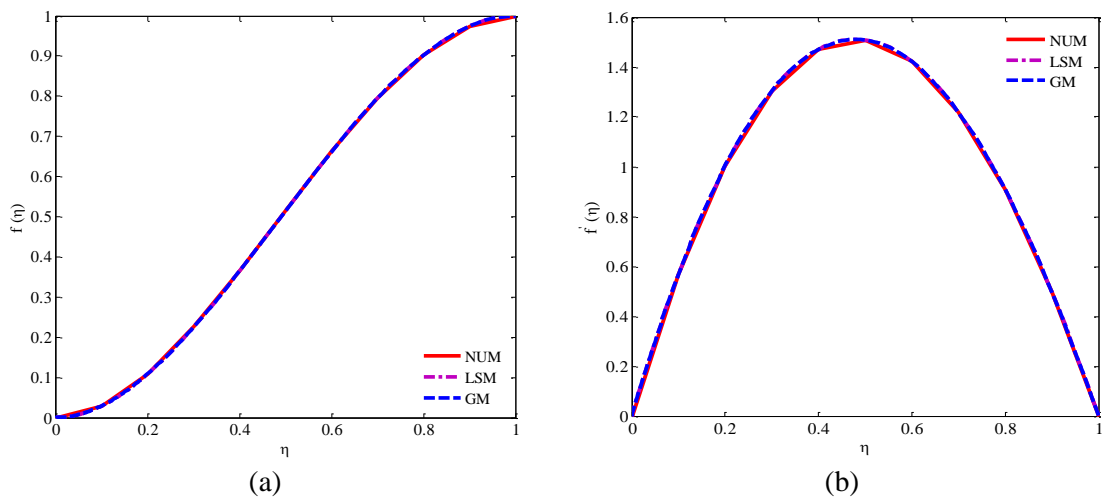

Fig.5. Comparison of the velocity components of numerical and analytical methods, a) f, b)f ' for k_1=0.01 and Re=0.5.
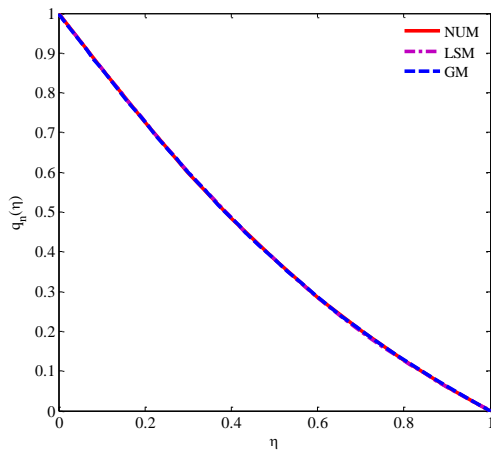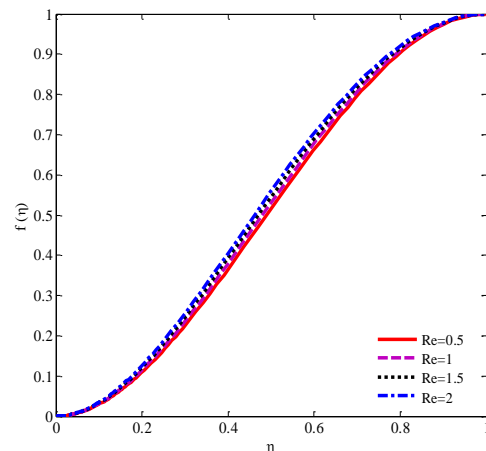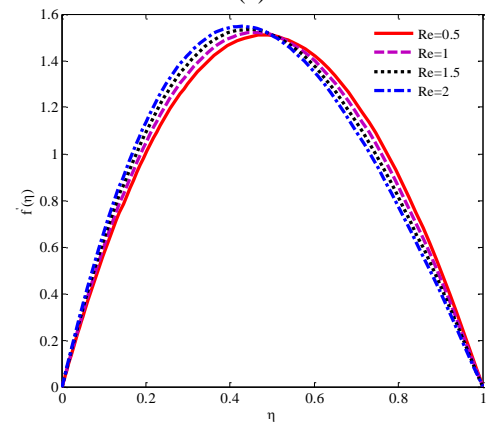
Fig. 6. Comparison of the temperature profiles of numerical and analytical methods (q_n), for k_1=0.01 and Re=0.5.

Figure 7 illustrates the effect of Reynolds number on the velocity profiles. As can be seen in this figure, by increasing velocity in the z direction, the Reynolds number increases. Also, the velocity in the r direction and near warm plate (z=0) increases and near the permeable wall (z=L) decreases. Also by increasing the Reynolds number, the maximum velocity value in the z direction approaches the warm plate. Although at low Reynolds numbers, the maximum value is taken place in the center of the channel. This change is due to intensify the velocity gradient near the warm plate and by increasing shear stress due to augmentation of the Reynolds number.

In Table 5 the effect of non-Newtonian fluid viscosity on the local friction coefficient ($f''(0)$) is examined. As can be seen, in constant k, by increasing the Reynolds number, $f''(0)$ increases, and because of the Reynolds number reflects the importance of the inertia effect to the effect of the viscosity, this conclusion is correct. Also, in a constant Reynolds number, by increasing the k, $f''(0)$ decreases, and due to the reduction of surface friction, using the viscoelastic fluid for cooling the gas turbine is recommended than Newtonian fluids.

(a)

(b)

Fig. 7. The effect of Reynolds number on the velocity components, a) f, b) f 'for $k_1 = 0.005$.

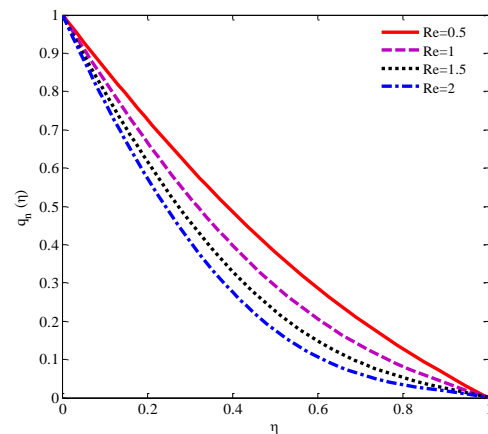Figure 8 indicates the effect of Reynolds number on the two-dimensional temperature distribution inside the channel.

Fig. 8. The effect of the Reynolds number on the temperature distribution components (q_n) for k_1=0.005, n = 2 and Pr = 1.

In low Reynolds numbers because of the laminar flow between the fluid layers, the parameter of temperature distribution along the z direction decreases continuously and in constant slope toward the permeable plate. But by increasing the Reynolds number the inertia effect is dominant than the effect of the viscosity, this uniform distribution disturbs and coolant inlet fluid, reducing the temperature at a constant η.

In Fig. 9, the effect of power law index on the temperature profile is shown. As can be seen, in a constant η by increasing power law index, the temperature value decreases. This indicates that the temperature distribution profile with low power law index calculates the temperature more than the actual amount and for estimating this problem temperature is not desired.

Figures 10 and 11 show the effect of the Prandtl number, Reynolds number and power law index on the Nusselt number. The Nusselt number is defined ($Nu = -q'_n(0)$). As can be seen with augmentation of the Prandtl number, the Nusselt number increases. According to the definition of the Prandtl number which is the thickness of the velocity boundary layer to the thermal boundary layer, increasing the Prandtl number means reducing thermal boundary layer thickness. Reducing the thickness of the thermal boundary layer means increasing the heat

transfer or in other word augmentation the Nusselt number. As shown in Fig. 11, by increasing the power law index, the Nusselt number increases. Indeed, the calculated temperature gradient in low power law index calculates the Nusselt number less than the actual value. Also by increasing the Reynolds number, the Nusselt number increases. Because increasing the Reynolds number causes the disturb augmentation of the thermal stratification on the heating plate and increases the heat transfer.
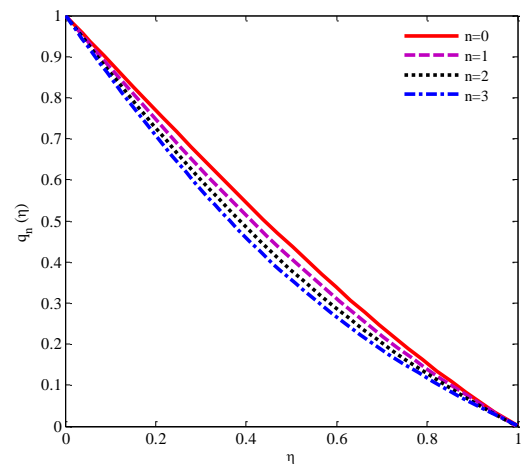

Fig. 9. Effect of n on temperature distribution component (q_n) for $k_1 = 0.005$, Re = 0.5 and Pr = 1.

Table 5. The effect of k_1 on friction surface (f '' (0)).

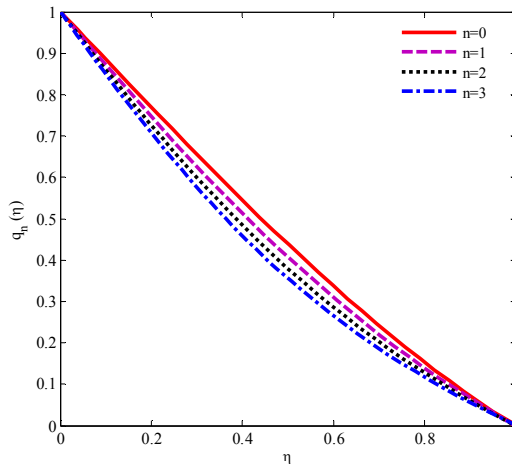| Re	k=0.0005	k=0.001	k=0.005	K=0.01
1	6.759073	6.757035	6.740617	6.719805
2	7.563378	7.529791	7.500940	7.463308
3	8.359470	8.300261	8.264010	8.215300
4	9.132730	9.063536	9.028690	8.981154

Fig. 10. Effect of n on temperature distribution component (q_n) for $k_1 = 0.005$, Re = 0.5 and Pr =1.
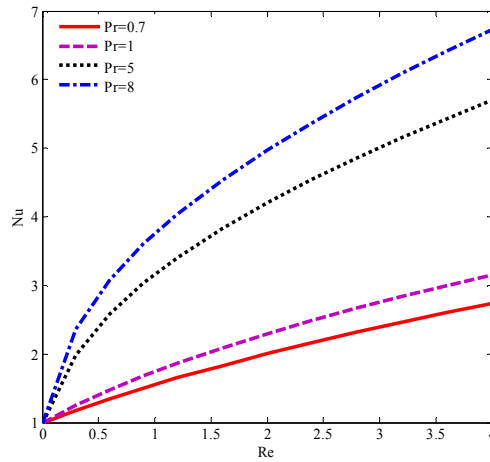

Fig. 11. Variations of the Nusselt number for different values of Pr at n=2 and $k_1 = 0.005$.

Table 6. The effect of k_1 on the Nusselt number for Pr=1and n=2.

Re	k=0.0005	k=0.001	k=0.005	K=0.01
1	1.998542	1.998563	1.998737	1.998962
2	2.743290	2.743509	2.745301	2.747659
3	3.376013	3.376643	3.379777	3.388768
4	3.936068	3.937253	3.947090	3.960340

Table 6 represents the effect of the Reynolds number and non-Newtonian fluid viscosity parameter on the Nusselt number. As already mentioned, increasing the Reynolds number leads to increase heat transfer, and thus increases the surface friction. Using the non-Newtonian fluid the amount of friction can be reduced to some extent. Also, it is observed that increasing the viscosity of the fluid conduces to an increase in the Nusselt number. For instance, the Nusselt number for k=0.005 and Re=4, and for k=0.01 and Re=4 have 0.6 percent discrepancy.

5. Conclusions

In this study, the methods of GM and LSM are used for solving the heat transfer problem of a non-Newtonian fluid flow in an axisymmetric channel with porous walls. Their conformity results with the numerical results in velocity and temperature profiles and tables are shown. The Galerkin method has further adaptation with the numerical results than the LSM. Then the effect of the Reynolds number, Prandtl number, power law index and non-Newtonian fluid viscosity on the flow and heat transfer are investigated. The results suggest that increasing the Reynolds number causes the augmentation velocity component. Also by increasing the Reynolds number, the maximum value of the f' diagram tends to warm plate. It is observed that the surface friction decreases with increasing viscosity. Also, the Nusselt number has a direct relationship to the Reynolds number.

References

[1] SW. Yuan, and AB. Finkelstein, "Laminar pipe flow with injection and suction through a porous wall", *Transaction of the ASME,* Vol. 78, No. 1, pp. 719-724, (1956).

[2] JL. White, and AB. Metzner, "Constitutive equations for viscoelastic fluids with application to rapid external flows", *AIChE Journal,* Vol. 11, No. 2, pp. 324-330, (1965).

[3] RM. Terill, "Laminar flow in a uniformly porous channel with large injection", *Aeronautics Q,* Vol. 16, No. 1, pp. 322-332, (1965).

[4] L. L. Debruge, and L. S. Han, "Heat transfer in a Channel with Porous Wall for Turbine Cooling", *Journal of Heat Transfer,* Vol. 94, No. 4, pp. 385-390, (1972).

[5] C. Kurtcebe, and M. Z. Erim, "Heat transfer of a non-Newtonian viscoinelastic fluid in an axisymmetric channel with a porous wall for turbine cooling application", *International Communication in Heat and Mass Transfer,* Vol. 29, No. 7, pp. 971-982 (2002).

[6] M. Esmaeilpour, G. Domairry, N. Sadoughi, and A.G. Davodi, Homotopy Analysis Method for the heat transfer of a non-Newtonian fluid flow in an axisymmetric channel with a porous wall", *Commun Nonlinear Sci Numer Simulat,* Vol. 15, No. 9, pp. 2424-2430, (2010).

[7] M. Hosseini, Z. Sheikholeslami, and D.D. Ganji, "Non-Newtonian fluid flow in an axisymmetric channel with porous wall", *Journal of Propulsion and power Research,* Vol. 2, No. 4, pp. 254-262, (2013).

[8] H. R. Ashorynejad, K. Javaherdeh, M. Sheikholeslami, and D.D. Ganji, "Investigation of the heat transfer of a non-Newtonian fluid flow in an axisymmetric channel with porous wall using Parameterized Perturbation Method (PPM)", *Journal of The Franklin Institute,* Vol. 351, No. 2, pp. 701-712, (2014).

[9] M. Hatami, and D. D. Ganji, "Heat transfer and flow analysis for SA-TiO$_2$ non-Newtonian nanofluid passing through the porous media between two coaxial cylinders", *Journal of Molecular Liquids,* Vol. 188, pp. 155-161, (2013).

[10] M. Hatami, and D. D. Ganji, "Thermal performance of circular convective–radiative porous fins with different section shapes and materials", *Energy Conversion and Management*, Vol. 76, pp. 185-193, (2013).

[11] M. Hatami, and D. D. Ganji, "Thermal and flow analysis of microchannel heat sink (MCHS) cooled by Cu–water nanofluid using porous media approach and least square method", *Energy Conversion and Management*, Vol. 78, pp. 347-358, (2014).

[12] M. Mollmahdi, M. Abbaszadeh, and G. A. Sheikhzadeh, "Flow field and heat transfer in a channel with a permeable wall filled with Al$_2$O$_3$-Cu/water micropolar hybrid nanofluid, effects of

chemical reaction and magnetic field", *Journal of Heat and Mass Transfer Research*, Vol. 3, No. 2, pp. 101-114, (2016).

[13] A. Vahabzadeh, M. Fakour, D. D. Ganji, and H. Bakhshi, "Analytical investigation of the one dimensional heat transfer in logarithmic various surfaces", *Alexandria Engineering Journal*, Vol. 55, No. 1, pp. 113-117, (2016).

[14] M. Fakour, D. D. Ganji, A. Khalili, and A. Bakhshi, "Heat Transfer in Nanofluid MHD Flow in a Channel With Permeable Walls", *Heat Transfer Research*, Vol. 48, No. 3, pp. 221-228, (2017).

[15] A. Rahbari, M. Fakour, A. Hamzehnezhad, M. Akbari Vakilabadi, and D. D. Ganji, "Heat transfer and fluid flow of blood with nanoparticles through porous vessels in a magnetic field: A quasi-one dimensional analytical approach", *Heat and Mass Transfer*, Vol. 283, pp. 38-47, (2017).

[16] R. H. Stern, and H. Rasmussen, "Left ventricular ejection: model solution by collocation and approximate analytical method", *Computers in Biology and Medicine,* Vol. 26, No. 3, (1996).

[17] B. Vaferi, V. Salimi, D. D. Baniani, A. Jahanmiri, S. Khedri, "Prediction of transient pressure response in the petroleum reservoisers using orthogonal collocation"*, Journal of Petroleum Science and Engineering,* Vol. 98-99, No. 1, pp. 156-163, (2012).

[18] F. A. Hendi, A. M. Albugami, "Numerical solution for Fredholm-Volterra integral equation of the second kind by using collocation and Galerkin methods", *Journal of King Saud University,* Vol. 22, No. 1, pp. 37-40, (2010).

[19] A. Aziz, and M. N. Bouaziz, " A least square method for a longitudinal fin

with tempreture dependent internal heat generation and thermal conductivity"*, Energy Conversion and Management,* Vol. 52, No. 8-9, pp. 2876-2882, (2011).

[20] M. Hatami, M. Sheikholeslami, and D. D. Ganji, "Laminar flow and heat transfer of nanofluid between contracting and rotating disks by least square method", *Powder Techonology,* Vol. 253, No. 1, pp. 769-779, (2014).

[21] M. Hatami, J. Hatami, and D. D. Ganji, "Computer simulation of MHD blood conveying gold nanoparticles as a third grade non-Newtonian nanofluid in a hollow porous vessel", *Computer Methods and Programs in Biomedicine,* Vol. 113, No. 2, pp. 632-641, (2014).

[22] M. Hatami, S. Mosayebidorcheh, and D. Jing, Two-phase nanofluid condensation and heat transfer modeling using least square method (LSM) for industrial applications", *Heat and Mass Transfer,* Vol. 53, No. 6, pp. 2061-2072, (2017).

[23] S. Mosayebidorcheh, M. A. Tahavori, T. Mosayebidorcheh, and D. D. Ganji, "Analysis of nano-bioconvection flow containing both nanoparticles and gyrotactic microorganisms in a horizontal channel using modified least square method (MLSM) ", *Journal of Molecular Liquids,* Vol. 227, pp. 356-365, (2017).

[24] R.S. Rivlin, "Plane strain of a net formed by inextensible cords, *Journal Rational. Mech,* Vol. 4, No. 2, pp. 323-425, (1995).

[25] R. C. Sherma, "Thermosolutal Convection in a Rivlin-Ericksen Rotating Fluid in Porous Medium in Hydromagnetics", *Indian Journal of Pure and Applied Mathematics*, Vol. 34, No. 1 , pp. 143-156, (2001).